Factors affecting the room-temperature mechanical properties of $TiCr_2$-base Laves phase alloys

Katherine C. Chen *, Samuel M. Allen, James D. Livingston

Massachusetts Institute of Technology, Department of Materials Science and Engineering, Cambridge, MA 02139, USA

Abstract

Various effects on the room-temperature mechanical properties of $TiCr_2$-base alloys have been assessed in efforts to improve the toughness of Laves phase intermetallics (AB_2). Systematic studies were performed on: (i) single-phase stoichiometric and nonstoichiometric $TiCr_2$, (ii) $TiCr_2$-base ternary Laves phases, and (iii) two-phase binary alloys containing $TiCr_2$. In order to make quantitative comparisons among the different alloys, Vickers indentation was used to obtain hardness and fracture toughness values. Within the single-phase field, constitutional defects accounted for the compositional dependencies of properties, and may aid the synchroshear deformation process. Ternary Laves phases comprised of Fe, Nb, V or Mo additions to $TiCr_2$ indicated that alloying elements which partition to both A and B sublattices can improve the toughness. Stabilization of the cubic $C15$ crystal structure also resulted in higher toughness values. Small amounts of the bcc β-phase effectively reduced crack lengths in the Laves phase, and two-phase alloys of (Ti,Cr) + $TiCr_2$ exhibited significant improvements in toughness.

Keywords: $TiCr_2$ alloys; Laves phases; Stoichiometry; Alloying; Mechanical properties

1. Introduction

Within the past decade, the class of Laves phase intermetallics (AB_2) has been explored to determine their potential as new structural materials. While several Laves phases have shown promise [1], brittleness remains to be the greatest limitation of these materials. Previous studies have offered various hypotheses for improving the toughness [2], but many of these ideas have not been systematically tested in a thorough and quantitative manner. Which factors affect the mechanical properties and to what extent they influence the properties need to be better established for the Laves phases.

The mechanical behavior of intermetallic compounds can be quite sensitive to composition, especially near the stoichiometric composition. Deviations from stoichiometry in the intermetallic NiAl result in increases in hardness and strength, and Ni vacancies were found to be more potent strengtheners per unit addition than Ni anti-site defects [3]. The deformation properties of the Laves phase $MgZn_2$ have been reported to be strongly dependent on the compositions within the range of homogeneity [4]. Due to the topological close-packing of atoms in Laves phases, defects associated with off-stoichiometric compositions may modify the atomic motions involved in the synchroshear deformation mechanism [1].

Reports of improved ductility or deformation in Laves phases alloyed with a third element include Ni added to $MgCu_2$ [5]; Mo to $SmFe_2$ [6]; Ti [7], V, or Mo [8] to $NbCr_2$; and Ti or Nb to HfV_2 [2,9]. The enhanced deformability demonstrated by HfV_2 with Nb additions has been proposed to be due to the alloying element residing on both the Hf and V sublattices, thereby 'opening up' the close-packed structure for easier atomic movements in the synchroshear mechanism [2,10]. The radius ratio, R_A/R_B, has been suggested to control the atomic free volume along the {111} shear planes in the $C15$ Laves structure [8].

In addition, alloying has also been proposed to lower the stacking fault energies of Laves phases, which might induce twinning and/or phase transformations upon deformation [2]. Low stacking fault energies are found

* Corresponding author. Present address: Los Alamos National Laboratory, Materials Science and Technology Division, Los Alamos, NM 87545, USA.

near crystal structure transition points, and stress-induced $C36-C15$ phase transformations have been reported in the $ZrFe_2$ Laves phase [11].

The brittleness of intermetallic alloys can be off-set with the incorporation of a second, more ductile phase [12–14]. Several two-phase Laves systems have been investigated, such as $Nb + NbCr_2$ [15,16], $Cr + NbCr_2$ [17–19], $Fe + NbFe_2$ [20], $Cr + HfCr_2$ [21], and $Fe + ZrFe_2$ alloys [11]. The Laves phase itself can experience some plastic deformation when contained within a large volume fraction of a second, more ductile phase [1]. For example, discrete $TiCr_2$ precipitates in a Ti-rich, two-phase structure have been observed with transmission electron microscopy (TEM) to deform by twinning and shear band formation [22].

The $TiCr_2$ Laves phase has been selected to study for numerous reasons. Promising mechanical properties and oxidation resistance at elevated temperatures have been reported for alloys containing $TiCr_2$ [23,24]. The Ti–Cr system also possesses some advantageous features to study the Laves phase. Most Laves phases form congruently or via eutectic or peritectic reactions, but $TiCr_2$ precipitates from a bcc solid solution. In addition, over 75% of the binary Laves phases are reported to be line compounds [25], yet a solubility range exists for $TiCr_2$. Thus, through appropriate annealing treatments, chemically-homogeneous, single-phase $TiCr_2$ can be formed over a range of compositions near stoichiometry. These samples are ideal to study the compositional dependencies of Laves phases. Some degree of microstructural control in the two-phase regions is also possible.

This paper surveys possible influences on the room-temperature mechanical properties of $TiCr_2$-base Laves phase alloys, with the goal of determining the best strategies for improving the toughness of Laves phase alloys. A series of experiments has been performed on $TiCr_2$-base alloys of different compositions and annealing treatments. The results are described in three sections of this paper: (i) single-phase stoichiometric and nonstoichiometric $TiCr_2$; (ii) single-phase, $TiCr_2$-base ternary Laves compounds; and (iii) two-phase binary alloys containing $TiCr_2$. Each of these sections presents a separate investigation into different effects on the toughness of $TiCr_2$. Direct comparisons of microhardness and fracture toughness values among all the alloys were possible via Vickers indentation.

The effects of defects accompanying nonstoichiometric Laves phase compositions are studied with the single-phase $TiCr_2$ alloys. A baseline of mechanical properties is also established for comparisons with the ternary Laves compounds and two-phase binary alloys. Ternary $TiCr_2$-base alloy compositions were selected so that the alloying element would be expected to occupy either the Ti-sublattice, the Cr-sublattice, or both sublattices. Changes in phase (crystal structure) stabilities, lattice constants, and solubility limits due to alloying are also studied and correlated with the mechanical properties.

Two-phase alloys containing $TiCr_2$ are the focus of the last section. A range of interesting microstructures has been revealed with different Ti–Cr alloy compositions and annealing treatments [26]. $TiCr_2$ in a large volume fraction of Ti-rich, bcc solid solutions and Cr-rich, bcc solid solutions are examined. Since the mechanical properties of the two-phase alloys are very dependent upon the microstructure, this treatment is a demonstration of changes that may occur when the Laves intermetallic is in a two-phase system. Indentation is again used to determine the microhardness and fracture toughness. Results are compared with the single-phase $TiCr_2$-base alloys from the previous sections and to other two-phase Laves systems.

2. Experimental procedures

The alloys were arc-melted using high-purity elements by the Materials Preparation Center of Ames Laboratory. The alloys were flipped and remelted several times to ensure homogeneity. The as-cast alloys had oxygen levels in the range of 82–178 ppm, and nitrogen levels of 20–46 ppm. The alloys were subjected to further homogenization treatments at 1395°C. Annealing treatments above 1200°C were performed in a vacuum furnace and oil-quenched. For the lower-temperature heat treatments, samples were encapsulated, annealed in a box furnace, and then water-quenched or air-cooled. Samples were wrapped in Ta foil to avoid oxidation during anneals. Alloy compositions were determined by electron microprobe analysis (EMPA), while crystal structures and lattice constants were determined by X-ray diffraction (XRD) using Cu–Kα radiation.

Due to the brittleness of Laves phases, room-temperature mechanical tests have been quite limited. Also, segregation, porosity, and/or microcracks from processing can influence the bulk property results. Microindentation offers the means to locally impart large deformation to a small, flaw-free test sample, thereby avoiding such problems. Several indentations can be made on a single specimen, and no machining of special sizes or shapes is required. The Vickers indentation technique was employed due to its simplicity and ability to provide information on both the flow and fracture of materials.

Cracks that emanate from the indentation impression corners provide data on the resistance to fracture. Average crack lengths (c) were determined by dividing the total lengths of all the radial cracks by four to represent an 'average' crack at each impression corner. The fracture toughness, K, was calculated by an equa-

Table 1
Microstructures, compositions, and crystal structures of the binary alloy samples near the $TiCr_2$ composition

Nominal alloy composition	Alloy microstructure	EMPA-Laves composition (1200°C)	Laves crystal structure		
			1300°C	1200°C	1000°C
Ti–62 Cr	β-Ti(Cr)+$TiCr_2$	Ti–(63.57 ± 0.08) Cr	*C*14	*C*36	*C*15
Ti–64 Cr	$TiCr_2$	Ti–(63.60 ± 0.12) Cr	*C*14	*C*36	*C*15
Ti–66 Cr	$TiCr_2$	Ti–(65.22 ± 0.07) Cr	*C*14	*C*36	*C*15/*C*36
Ti–67 Cr	$TiCr_2$	Ti–(66.06 ± 0.06) Cr	*C*14	*C*36	*C*36
Ti–68 Cr	β-Cr(Ti)+$TiCr_2$	Ti–(66.30 ± 0.03) Cr	*C*14	*C*36	*C*36
Ti–69 Cr	β-Cr(Ti)+$TiCr_2$	Ti–(66.31 ± 0.04) Cr	*C*14	*C*36	*C*36

tion developed by Anstis et al., which is based on elastic/plastic indentation fracture mechanics [27]:

$$K = 0.016(E/H)^{1/2}(P/c^{3/2})$$

where H is the hardness value, P is the load in kilogram-force, and c is the average crack length. A Young's modulus value (E) of 235 GPa was used [7].

Samples for microindentation were fine polished with a colloidal 0.05 μm alumina suspension solution in order to remove any compressive surface stresses that may form during sample preparation and that can reduce crack lengths that result in faulty and nonreproducible toughness measurements [28]. An indentation load of 500 g was generally used and applied for about 12 s. At least five to ten indentations were made on each sample. Impression diagonals and crack lengths were measured with an environmental scanning electron microscope (SEM) at high magnifications. Indentations with lateral cracks, or spallation, were generally avoided in the measurements, unless they were truly representative of the alloy behavior. Consistent testing and measurement conditions were made for fair comparisons among the different alloy samples.

3. Results and discussion

3.1. Single-phase $TiCr_2$

3.1.1. Nonstoichiometry defects

Six binary alloy compositions ranging from Ti–62 at.% Cr to Ti–69 at.% Cr were selected to study the single-phase $TiCr_2$ Laves field. Off-stoichiometry in $TiCr_2$ was found only towards the Ti-rich compositions, and the single-phase field is quite small, roughly Ti–64 at.% Cr to Ti–67 at.% Cr. Three of the alloy samples fell within the two-phase regions and contained small amounts (less than 10 vol.%) of the bcc β-phase. A previous study [29] details the microstructural investigation of these alloys, and is summarized in Table 1. Identification of the defect mechanism accompanying nonstoichiometry is important to understand the compositional trends in the mechanical properties. A combination of metallography, X-ray diffraction, lattice constant measurements, density measurements, and electron microprobe analysis was used, and results suggested that the nonstoichiometry in $TiCr_2$ is accommodated by both anti-site substitutions and vacancies [29].

3.1.2. Microhardness

Vickers indentations were performed on the six binary alloy samples after several different heat treatments. Since the crystal structure of $TiCr_2$ is dependent upon the annealing temperatures (Table 1), different Laves crystal structures at the same composition were also studied. Fig. 1 plots all the microhardness data points based on alloy composition and crystal structure.

The single-phase *C*14 alloys showed no distinctive microhardness variation with alloy composition. Since the grain sizes were much larger than the indentation size, the indentations were effectively on single crystals of unknown orientations, and thus anisotropies of this hexagonal phase may have masked any compositional

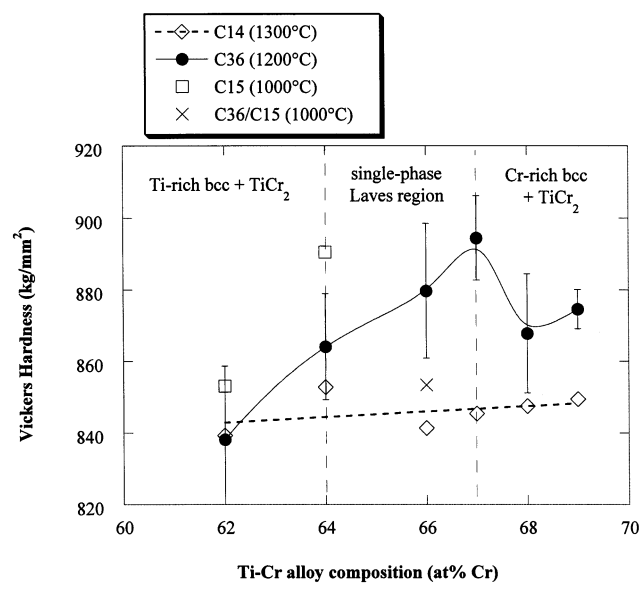

Fig. 1. Alloy composition and crystal structure dependence of microhardness values of the single-phase (or nearly so) $TiCr_2$ alloys.

influences. However, the $C36$ alloys did exhibit a compositional dependence on hardness (as shown by the curve in Fig. 1), with the maximum hardness at the composition closest to stoichiometry. This dependence resulted with measurements made at two different Vickers indentation loads and with Knoop indentation [30]. The decrease in hardness in the two-phase alloys (outside the Ti-64–67 at.% Cr range) can be attributed to small amounts of the softer bcc β-phase.

Because the $C15$ structure was not uniformly achieved in all the alloy samples (see Table 1 and [29]), the composition dependence of hardness in $C15$ $TiCr_2$ could not be determined directly. However, the Ti-rich, two-phase alloys with the $C15$ structure have higher hardness values than the corresponding hexagonal structures at the same alloy compositions, suggesting that the $C15$ structure has the highest hardness. The Ti–66 Cr alloy at 1000°C had a mix of $C36$ and $C15$ structures, and appears to have a much lower hardness. Thus, the $TiCr_2$ Laves phase hardness is not only dependent upon the composition, but also the crystal structure.

The observed hardness behavior in the $C36$ single-phase Laves region contradicts the usual trend found in intermetallics. Westbrook [31] has documented that in several intermetallic systems, the stoichiometric composition has the lowest hardness, and increasing off-stoichiometric compositions show increased hardness at low homologous temperatures. The defects in the non-stoichiometric compounds are thought to interfere with dislocations, and thus produce hardening. At higher homologous temperatures, these defects then have a softening effect since diffusion rates are enhanced and dislocation climb becomes easier.

On the other hand, Paufler et al. [32,33] documented a similar maximum hardness at the stoichiometric compositions of $MgZn_2$ and $NbFe_2$ Laves phases. The defects associated with off-stoichiometry were shown to decrease the mobility of the dislocations, but the dislocation density also increased to produce the overall decrease in hardness. Therefore, the class of Laves phase intermetallics appears to behave differently than other intermetallics with simpler structures.

3.1.3. Fracture toughness

The fracture toughness values of the $TiCr_2$ alloys are plotted in Fig. 2. Different crystal structures and alloys with varying amounts of a second phase are plotted together. Within the single-phase region, the values for fracture toughness are quite low. The $C15$ structure at Ti–64 Cr shows a significant increase in toughness over the hexagonal structures ($C36$ and $C14$) at the same alloy composition. The cubic structure may offer more deformability due to the additional crystal symmetry and the greater number of available slip systems. In addition, the cubic $C15$ Laves phase can also deform

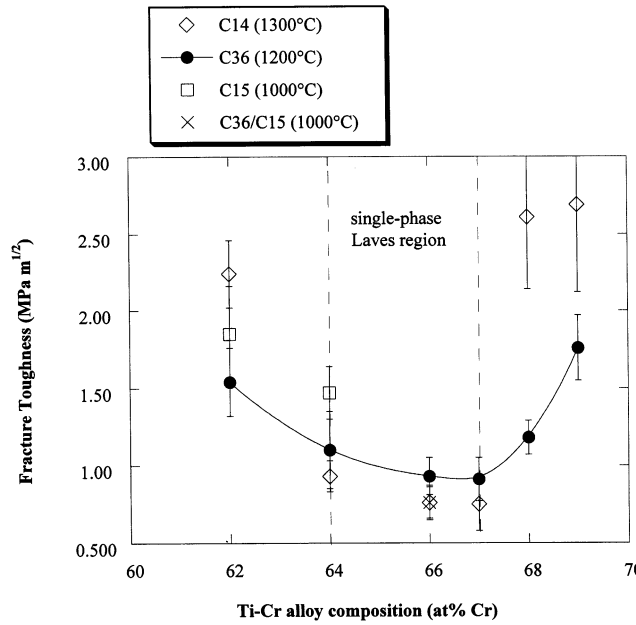

Fig. 2. Alloy composition and crystal structure dependence of fracture toughness values of the single-phase (or nearly so) $TiCr_2$ alloys.

by twinning, as seen in the $TiCr_2$ precipitates in Ti-rich, two-phase binary alloys [22]. Alloying the Laves phases to stabilize the cubic $C15$ structure will be discussed in a later section.

The Ti–66 Cr alloy annealed at 1000°C contained a mixture of the $C15$ and $C36$ structures, and provided a test sample for potential stress-induced phase transformations, or 'transformation toughening'. Alloys exhibiting polytypism are thought to have low stacking fault energies, which may enhance twinning [2]. In $ZrFe_2$, embryos of $C15$ in the $C36$ Laves alloy were discovered to grow upon applied stress from room-temperature compression [11]. However in this particular $C36/C15$ $TiCr_2$ sample, the low fracture toughness does not reflect such a mechanism occurring.

Fig. 2 also shows the compositional dependence of the fracture toughness in the $C36$ $TiCr_2$ alloys. The minimum fracture toughness value occurs nearest the stoichiometric $TiCr_2$ composition. Within the single-phase Laves field, slight increases in the fracture toughness were found with increased deviation from stoichiometry. Disorder in the off-stoichiometric compositions (from excess Ti and/or Cr vacancies) results in greater toughness. More faults and dislocations may exist in these alloys, which allow for greater deformation. The lower hardness values of the off-stoichiometric compositions are consistent with this idea.

Vacancies have been proposed to assist the movement of synchro-Shockley dislocations [34]. Plasticity in the Laves phases relies on the motion of these dislocations to produce slip, twinning, and phase transformations. A Shockley dislocation can have its core split

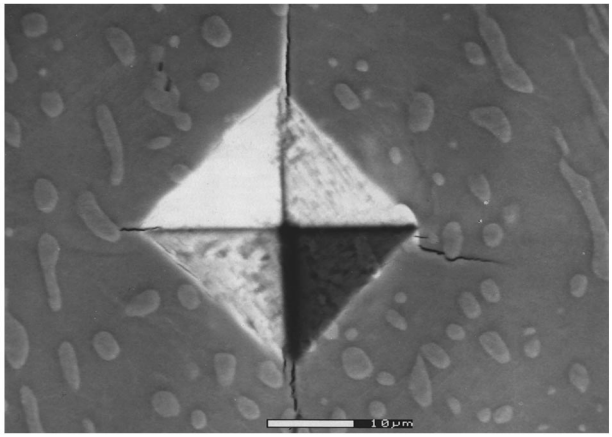

Fig. 3. SEM micrograph of radial cracks disrupted by or terminated at the β-bcc phase particle in the Ti–69Cr alloy.

over two closely-spaced planes. At the core, atoms must swap positions, and vacancies are believed to facilitate this process. A vacancy moving along with a kink in a dislocation enables the atomic interchange to take place without much dilatation of the crystal. Currently, there is no direct evidence that vacancies are involved with the motion of synchro-dislocations, but on the whole, experimental work on the Laves phases show that phase transformations tend to be sluggish and plasticity normally occurs only at temperatures greater than about two-thirds the melting temperature. At these higher temperatures, the dislocations have greater mobility, which can be assisted by vacancies. Furthermore, the trends displayed in this indentation study of the single-phase $TiCr_2$ alloys are entirely consistent with such a postulate. The off-stoichiometric alloys, which are thought to possess vacancies [29], exhibit decreased hardness and increased fracture toughness compared to the stoichiometric $TiCr_2$ sample. Thus, the improved deformability in the off-stoichiometric compositions can be explained by the presence of vacancies assisting the synchroshear deformation process.

Marked improvements in the fracture toughness are displayed by the alloys that fall in the two-phase fields, and are due to the dispersed, more ductile β phase. The substantial increase in toughness in the Cr-rich *C*14 alloys after annealing at 1300°C stems from the numerous dispersed β-particles present due to the higher equilibrium volume fraction of the β-phase than the same alloy composition after annealing at 1200°C. Radial cracks were often disrupted by or terminated at the β-phase particles, as seen in Fig. 3. The more ductile phase allows crack deflection and crack bridging. The second phase may also absorb some of the crack energy by the formation of a plastic zone at the crack tip. High magnification of cracks in the two-phase alloys revealed that the cracks often circumvented the β-particle, indicating bcc/Laves phase interface debonding. Some deformation energy may be relieved by the debonding of interfaces [35], which leads to improved toughness values.

The increases in toughness with small amounts of a second, more ductile phase are much greater than those arising from nonstoichiometry in the single-phase $TiCr_2$ Laves phase compositions, or from variations in the crystal structure. Section 3.3 discusses the properties of alloys with large volume fractions of the bcc phase.

3.2. Ternary $TiCr_2$-base Laves phases (single-phase)

3.2.1. Alloying elements and site occupancy

In order to investigate the effects of sublattice site substitutions, specific alloying elements were chosen to substitute for the Ti atom, the Cr atom, and both atoms simultaneously. Changes in the equilibrium crystal structure also occur with the alloying additions, due to changes in the electron concentration and stacking fault energies [36]. Four alloying elements were selected on the basis of atomic radius [37], electronegativity [38], other Laves phases formed, and the available ternary phase diagrams in the literature. Table 2 lists the ternary alloys studied with the proposed atomic site occupancy and crystal structure stabilization.

Fe has a smaller radius than Cr and a continuous $TiCr_2$–$TiFe_2$ solid solution exists [39,40], indicating that Fe will most likely substitute for the Cr atom. Likewise, Nb will substitute primarily for Ti due to Nb's slightly larger radius than Ti and due to the continuous solid solution between $TiCr_2$ and $NbCr_2$ [41]. Neither V nor Mo forms a Laves phase with Ti or

Table 2
Possible sublattice sites and crystal structure stabilization of aloying elements in tenary $TiCr_2$-base Laves phase based on radius, electronegativity and other Laves phases formed

Element	Radius (Å)	Electronegativity	Other Laves phases	Possible sublattice	Ternary Laves compound	Phase stability
Ti	1.46	1.3				
Nb	1.47	1.35	$NbCr_2$	Ti	$(Ti,Nb)Cr_2$	*C*15
V	1.35	1.75	—	Ti,Cr?	$(Ti,V)(V,Cr)_2$?	*C*15, bcc
Mo	1.40	1.85	—	Ti,Cr	$(Ti,Mo)(Mo,Cr)_2$	*C*15, bcc
Fe	1.27	1.85	$TiFe_2$	Cr	$Ti(Fe,Cr)_2$	*C*14
Cr	1.28	1.7				

Cr, and both V and Mo are intermediate in size with Ti and Cr. These two elements were selected as possible candidates to occupy both Ti and Cr sublattices. The nominal alloy compositions of different Ti–V–Cr and Ti–Mo–Cr alloys were designed to test the capacity to accommodate the alloying element preferably on one sublattice over another, and to examine the solubility limits of the ternary Laves phases.

The ternary alloys were first characterized in terms of microstructures, solubility limits, and crystal structures. Microprobe analysis and lattice constant measurements were used to help establish or confirm the sublattice site occupancies of the alloying elements. The Ti–Fe–Cr Laves phase composition determined by EMPA confirmed that the Fe atoms replaced the Cr atoms to form single-phase $Ti(Fe,Cr)_2$ ternary Laves compounds. Additions of Fe to $TiCr_2$ were also found to decrease the unit cell volume.

Similarly, Nb atoms replaced the Ti atoms along the continuum of $TiCr_2$ to $NbCr_2$. As the Nb concentration increased, the lattice constant increased and the $C14$–$C15$ transition temperature increased (which is to be expected since $NbCr_2$ has a higher transition temperature than $TiCr_2$). XRD studies showed that the additions of Nb to $TiCr_2$ stabilized the $C15$ crystal structure. Compositions determined by EMPA of the Laves phase in the Ti–Nb–Cr alloys were consistently at 66 at.% Cr, indicating that $(Ti,Nb)Cr_2$ ternary Laves phases were formed.

V and Mo were selected to replace both the Ti and Cr atoms. Since the solubilities of V and Mo in $TiCr_2$ are quite small and the binary $TiCr_2$ Laves phase is not a strict line compound, the analysis for the sublattice site of V and Mo in $TiCr_2$ was more difficult. Some of the V and Mo ternary alloys also contained small amounts of the β-phase, indicating that the solubility limits had been exceeded. A plot of the lattice constant versus the Cr/Ti composition ratio (Fig. 4) was used to help determine the sublattice occupancy of V and Mo. If the alloying element replaces the Cr atoms, the Cr/Ti composition ratio decreases, and since the alloying element is larger than Cr (and smaller than Ti), the ternary Laves phase lattice constant should increase. Meanwhile, the replacement of Ti atoms would result in a higher Cr/Ti composition ratio and a smaller lattice constant.

The Mo alloys span the Cr/Ti composition ratio range, and display lattice constants larger and smaller than $TiCr_2$. Thus, Mo can replace both the Ti and Cr atoms in $TiCr_2$, and one can have a range of atomic site replacements (where the Mo atoms substitute mostly on the Ti-sublattice, the Cr-sublattice, or equally on both). The nominal alloy composition forces the Mo atoms onto either the Ti sublattice or Cr sublattice. However, V alloys are consistently seen to have Cr/Ti composition ratios less than 2.0 and have lattice constants larger than the binary $TiCr_2$. Thus, most of the V atoms must occupy the Cr sites as $Ti(V,Cr)_2$ ternary Laves phases. Similarly, Chu et al. [42] have found V to substitute primarily on the Cr-sublattice in $NbCr_2$ by electronic calculations and atom location channeling enhanced microanalysis (ALCHEMI).

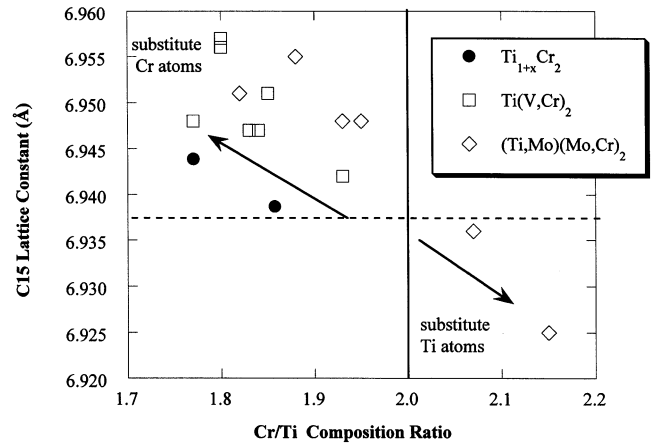

Fig. 4. The Cr/Ti composition ratio vs. the $C15$ lattice constant. The lattice constant increases and Cr/Ti decreases when V or Mo substitutes on the Cr-sublattice. The lattice constant decreases and Cr/Ti increases when substituting on the Ti-sublattice.

3.2.2. Indentation

Microhardness of the single-phase ternary Laves compounds are plotted in Fig. 5 and the fracture toughness is plotted in Fig. 6 as a function of the concentration of 'alloying element'. (Alloy addition is set in quotes because nonstoichiometric binary $C36$ $TiCr_2$ data points from the last section are included, and excess Ti atoms and/or Cr vacancies are treated as 'alloy additions' to $TiCr_2$.) Table 3 lists all the alloy compositions, microstructures, crystal structures, lattice constants, and mechanical properties. Despite the large scatter in the data, the differences and trends among the alloys were reproducible and are believed to be real.

The $Ti(Fe,Cr)_2$ ternary alloys all showed a decrease in hardness value and a large decrease in fracture toughness compared to the binary $C14$ $TiCr_2$ (not all data points are plotted). The $(Ti,Nb)Cr_2$ alloys revealed that increasing the Nb-content increased the hardness values, while the toughness gradually decreased.

The single-phase $Ti(V,Cr)_2$ and $(Ti,Mo)(Mo,Cr)_2$ alloys have slightly higher hardness values than the binary $TiCr_2$ alloys. The ternary alloys with small amounts of the bcc phase (not shown in the plots) have slightly lower hardness but higher toughness values. Alloys with a $C15/C36$ structure also showed a lower hardness than those with the $C15$ structure. These trends were also found with the binary $TiCr_2$ Laves alloys near stoichiometry.

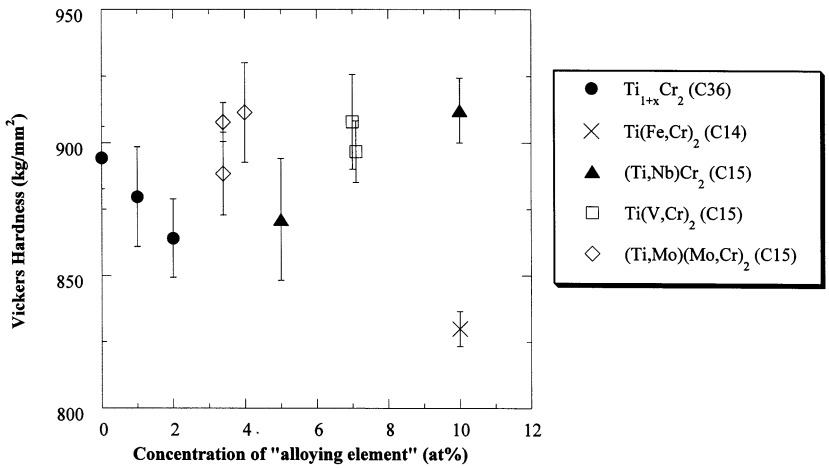

Fig. 5. Concentration of 'alloying element' to $TiCr_2$-base Laves alloys (single-phase) vs. the Vickers hardness (at a load of 500 g).

The Mo alloys had slightly higher toughness values, and the V alloys exhibited roughly 25% improvements over the binary $TiCr_2$ alloys. These improvements in toughness occurred with fairly small concentrations of the alloying element (which were also the maximum solubility in $TiCr_2$). Thus, the toughness of Laves phases can be improved through appropriate alloying. Greater gains in toughness may be possible with greater solubility of alloying elements in Laves phases. Other Laves systems and processing techniques may extend the solubility limits for better toughening opportunities.

As concluded in Section 3.1, the mechanical properties of Laves phases are influenced by the crystal structure, defect structures, and the presence of small amounts of another phase. The alloying additions add to the complexity of factors that affect the mechanical properties, such as alloying element size, electronegativity, and sublattice site occupancy. In addition, other constitutional defects (such as vacancies) may be present and remain unidentified in these ternary alloys. Fleischer [43] describes several different possible defects that may form from ternary substitutions and notes that their combined effects on properties are difficult to predict. However, he concludes that primary strengthening comes from the familiar elastic forces between point defects and moving dislocations, arising from size and modulus interactions.

Some of the observed changes in hardness and fracture toughness can be correlated with changes in the lattice constants (and thus indirectly with the sublattice-site occupancy of the alloying element). Laves phases (AB_2) are often referred to as 'size-factor' compounds that have a close-packed structure with an ideal radius ratio of the A atom to the B atom of 1.225. In a rigid-sphere model, this radius ratio enables spheres of the same size to be in contact with each other, while spheres of different sizes do not have any contact. However, Laves phases actually exist with a range of radius ratios, from 1.05 to 1.68. Atoms are thought to expand or contract accordingly to reach the ideal ratio, which may introduce A–B contacts, as well as internal strain [44]. The $TiCr_2$ Laves phase has a radius ratio of 1.14, which falls well below the ideal value. Following Pearson's dimensional analyses [45], the first interatomic contacts to be made are by the Cr atoms, and therefore the unit cell dimensions are controlled by the Cr–Cr contacts. The Cr-sublattice undergoes compression in order to achieve the optimum packing dictated by geometrical considerations.

Large changes in the unit cell dimensions (i.e. the lattice constant), can therefore be affected by substitution on the Cr-sublattice. Excess Ti on Cr-sites has already been seen to increase the lattice constant in the binary alloys [29]. The smaller Fe atoms on the Cr-sublattice of the $Ti(Fe,Cr)_2$ alloys cause the unit cell to decrease with Fe-content. Possibly, the effect of Fe contracting the unit cell puts the B-sublattice under further compression and causes the Laves phase to become less crack resistant, or more brittle.

Nb is slightly larger than Ti, and at 5 at.% Nb the lattice constant remains unchanged within experimental error, and only at larger concentrations of Nb does the lattice constant increase. Thus replacing the A atoms in a lattice controlled by the B–B contacts has a smaller effect than replacing the B atoms. The hardening effect seen in the 10 Nb alloy and not the 5 Nb alloy parallels the changes in the lattice constant for the $(Ti,Nb)Cr_2$ alloys. Solid-solution hardening in intermetallics occurs due to lattice strains from alloying, although other factors may play a role as well [46].

Thus, the role of sublattice-site occupation by the alloying element may have significance in that the lattice size can be affected. Selection of the appropriate alloying element on particular sublattices can either increase or decrease the unit cell. Nb added to HfV_2 was suggested to improve the deformability because Nb

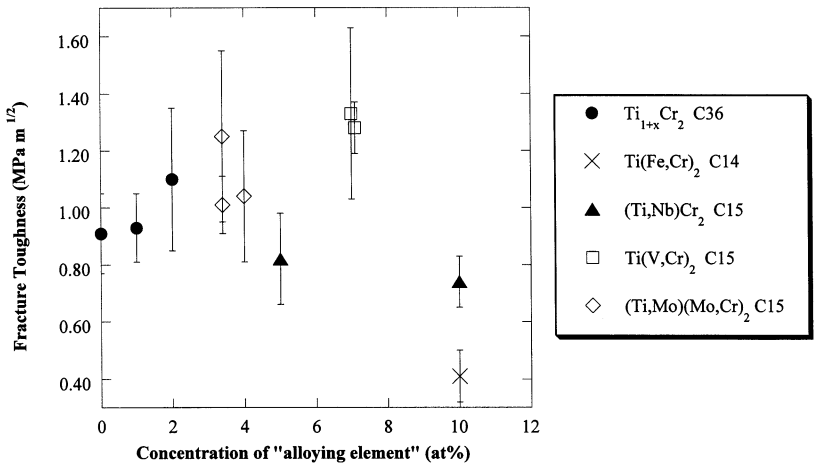

Fig. 6. Concentration of 'alloying element' to $TiCr_2$-base Laves alloys (single-phase) vs. the fracture toughness determined by indentation.

'opened up' the lattice [2,10]. The disruption of the tight close packing of atoms in the Laves phase may enable easier atomic movements involved in the synchroshear deformation process. From this study, the V additions to $TiCr_2$ increased the lattice constant and improved the fracture toughness. However, such correlation has not been proven, and the general rule of selecting an alloying element that resides on both sublattices of a Laves phase to improve ductility warrant further investigations. The enticing toughening effects seen in HfV_2 may be more complicated (possibly due to a lattice instability or superconducting transition), and not generally applicable to all other Laves systems.

A significant influence of the alloying elements on the mechanical properties of $TiCr_2$ comes through the ability to stabilize certain crystal structures. Alloying elements can increase or decrease the electron concentration of Laves phases, and thereby affect stacking fault energies and the phase (crystal structure) stability. Nb, V, and Mo all extended the equilibrium $C15$ region of $TiCr_2$, and the $C15$ structure has consistently shown the highest hardness and toughness values. The $C14$ Fe ternary alloys were the most brittle samples in this study. The large number of slip systems associated with cubic structures may inherently offer greater deformability and toughness than the hexagonal Laves crystal structures. Many investigators employ this fact for other intermetallic systems. The VCo_3 intermetallic with a low-symmetry hexagonal structure has been alloyed with Fe to transform into the higher symmetry cubic $L1_2$ structure for improved ductility [47]. Similarly, $TiAl_3$ that has been alloyed with Mn and Cr to change the tetragonal DO_{22} crystal structure to the $L1_2$ structure, has been shown to improve crack resistance [48].

Solubility limits were also affected by the alloying elements V and Mo, as many of the alloys (unexpectedly) had a fine two-phase microstructure. Again, the presence of a second, more ductile phase can greatly improve the fracture toughness without sacrificing much of the strength of an alloy. Thus, the appropriate alloying element may improve the toughness of the Laves phase itself, and may also induce the precipitation of a second phase that could further improve the toughness of the whole alloy system. On the other hand, alloying may also extend the solubility limits of the Laves phase field, and offer more toughening opportunities. As seen from the last section, toughness improved with deviation from the stoichiometric Laves composition.

3.3. *Two-phase alloys containing $TiCr_2$*

3.3.1. *Microstructures*

Two alloys each were selected on the Ti-rich side (Ti–30 Cr, Ti–40 Cr) and the Cr-rich side (Ti–80 Cr, Ti–87.5 Cr) of the $TiCr_2$ composition. The as-cast binary alloys were generally single-phase bcc β. Upon annealing, the different nominal compositions of the Ti–Cr alloys produced very different microstructures of (Ti,Cr)-bcc + $TiCr_2$ and are described in detail elsewhere [26]. The Ti-rich alloys contained discrete precipitates of the $TiCr_2$ Laves intermetallic (Fig. 7), while the Cr-rich alloys displayed fine, eutectoid-like microstructures (Fig. 8(a)). Processing and annealing treatments can influence the microstructures of two-phase Laves alloys in order to achieve certain properties, as several other investigators have explored [17,21].

3.3.2. *Microhardness*

Indentation on the two-phase alloys was performed at a load of 500 g for consistency with the previous sections and also to ensure that the representative dual-phase microstructure was being sampled, rather than

Table 3
Microstructures, crystal structures, lattice constants and mechanical properties of the $TiCr_2$-base Laves phase alloys

Nominal alloy composition	Alloy microstructure	Crystal structure	Laves lattice constant (Å)	Hardness (kg mm^{-2})	Toughness (MPa $m^{1/2}$)
Ti–67 Cr (1300°C)	Single-phase	*C*14	6.935[a]	845 ± 13	0.75 ± 0.17
Ti–67 Cr (1200°C)	Single-phase	*C*36	6.932[a]	894 ± 12	0.91 ± 0.14
33Ti–10Fe–57Cr (1300°C)	Single-phase	*C*14	6.914[a]	830 ± 07	0.41 ± 0.09
33Ti–20Fe–47Cr (1300°C)	Single-phase	*C*14	6.880[a]	827 ± 14	0.40 ± 0.08
28Ti–05Nb–67Cr (1200°C)	Single-phase	*C*15	6.9388	871 ± 23	0.82 ± 0.16
23Ti–10Nb–67Cr (1200°C)	Single-phase	*C*15	6.9455	912 ± 12	0.74 ± 0.09
18Ti–15Nb–67Cr (1200°C)	Single-phase	*C*15	6.9536	914 ± 19	0.69 ± 0.03
31.8Ti–4.5V–63.7Cr (1200°C)	Fine β precipitates	*C*15/*C*36	6.947	857 ± 19	1.28 ± 0.23
31.8Ti–4.5V–63.7Cr (1000°C)	Fine β precipitates	*C*15	6.942	880 ± 31	1.20 ± 0.16
32Ti–7V–61Cr (1300°C)	Single-phase	*C*15	6.948	908 ± 18	1.33 ± 0.30
32Ti–7V–61Cr (1000°C)	Single-phase	*C*15	6.947	897 ± 12	1.28 ± 0.09
34Ti–4Mo–62Cr (1200°C)	Fine β precipitates	*C*15/*C*36	6.955	868 ± 13	1.30 ± 0.20
34Ti–4Mo–62Cr 1000°C)	Fine β precipitates	*C*15	6.951	880 ± 25	1.14 ± 0.25
32Ti–4Mo–64Cr (1200°C)	Single-phase	*C*15/*C*36	6.948	888 ± 16	1.01 ± 0.10
32Ti–4Mo–64Cr (1000°C)	Single-phase	*C*15	6.948	908 ± 07	1.25 ± 0.30
30Ti–4Mo–66Cr	Fine β precipitates	*C*15/*C*36	6.936	867 ± 44	1.13 ± 0.18
30Ti–4Mo–66Cr (1000°C)	Single-phase	*C*15	6.925	911 ± 19	1.04 ± 0.23

[a] Adjusted lattice constant for hexagonal structures (cubed root of volume).

just individual phases. Fig. 7 displays an indentation impression sampling a representative region of the two-phase structure in a Ti-rich alloys. The hardness values of the β-phase are much lower than those of the Laves phase. The single-phase β ranged in hardness from about 400 to 550 kg mm^{-2}, with Cr-rich compositions being harder than Ti-rich compositions. Section 3.1 revealed the $TiCr_2$ Laves phases to have hardness values around 850–900 kg mm^{-2}.

Annealing the as-cast alloys resulted in the increases in hardness due to the precipitation of $TiCr_2$. In the Ti-rich alloys, low volume fractions of the Laves phase did not have much of a hardening effect, although a dense structure of fine $TiCr_2$ precipitates proved to be a potent strengthener. The two-phase structures in a Ti–40 Cr alloy had an almost 100 kg mm^{-2} increase in hardness from the as-cast condition. The larger $TiCr_2$ equiaxed precipitates in the Ti–40 Cr alloy showed some cracking after indentation. A critical size of the Laves phase precipitate appeared to be necessary for cracking.

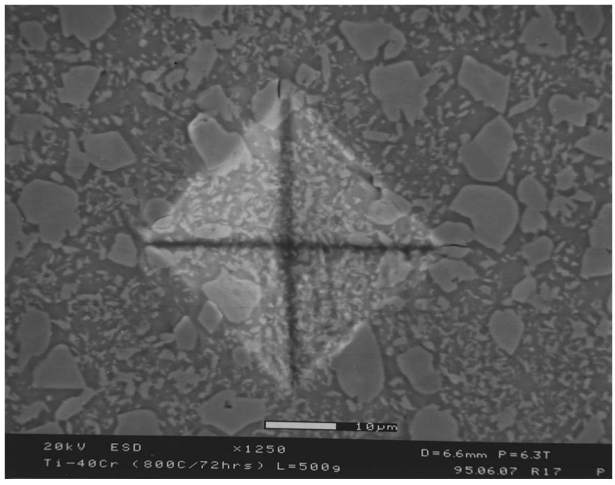

Fig. 7. Microhardness indentation on a Ti–40 Cr alloy annealed at 800°C. The discrete, lighter phase is the $TiCr_2$ Laves phase intermetallic.

The Cr-rich alloys exhibited higher hardness values than the Ti-rich alloys. Fig. 9 plots the hardness value versus the Laves phase volume fraction, and takes the *C*36 stoichiometric value for $TiCr_2$. The dotted line represents the rule of mixtures hardness values between single-phase β at Ti–87.5 Cr and single-phase *C*36 $TiCr_2$ (the two phases by the tie-line at 1200°C). The Ti–80 Cr alloy annealed at 1200°C, with 35 vol.% of the Laves phase, had a microhardness value higher than the rule of mixtures predicts. The strengthening effect also comes from the fine, two-phase microstructure. The high microhardness values of 700–750 kg mm^{-2} of the annealed Ti–80 Cr alloys are quite appealing, considering that no cracks were formed at a load of 500 g.

3.3.3. Fracture toughness

The attractiveness of the Cr-rich, two-phase alloys with high hardness and no cracking motivated the attempt to measure the fracture toughness of these alloys. In order to allow comparisons with the other $TiCr_2$-base alloys from the earlier sections, indentation with a higher load was employed to produce indentation cracks, rather than using a totally different method (such as bend tests). A large Vickers indenter was

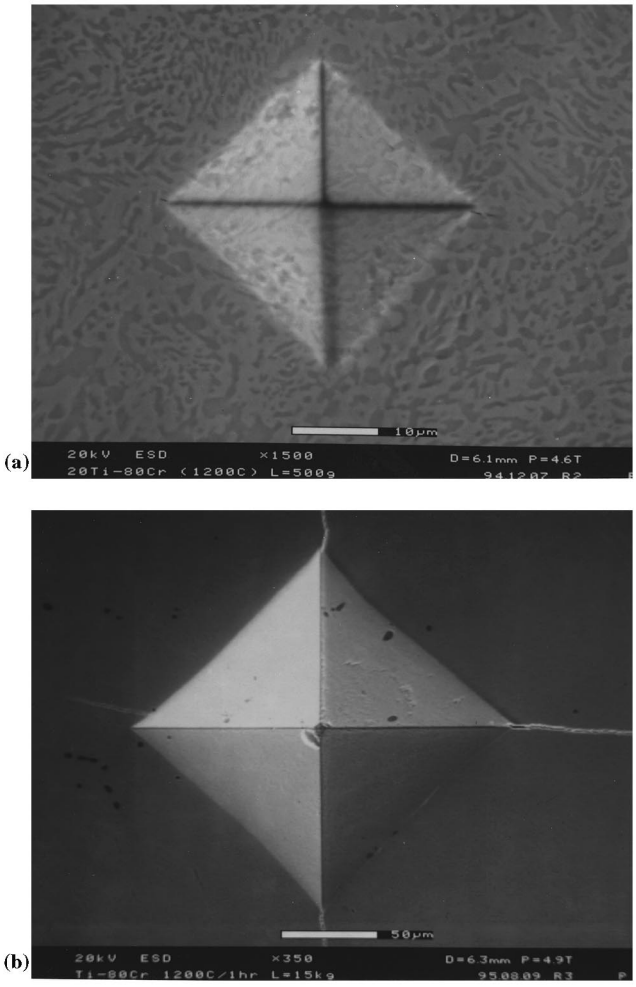

Fig. 8. The Ti–80 Cr alloy annealed at 1200°C with indentations at loads of (a) 500 g and (b) 15 kg. Cracks are produced with only high loads.

attached to a Rockwell superficial hardness tester to generate the larger loads. Hardness values using a 15 kg load were only 3–4% less than values obtained using a 500 g load (and close to the standard deviation value). Thus measurements obtained with this hardness tester were comparable to those obtained with the microhardness tester.

Fig. 8(a) and (b) show the indentation of the Ti–80 Cr alloy annealed at 1200°C at the 500 g load and the 15 kg load, respectively. Cracks formed only with the higher indentation load. The annealed Ti–87.5 Cr alloy contained low volume fractions of the Laves phase and did not show cracking. A higher critical load would be required to initiate cracks. The Ti-rich, two-phase alloys also did not experience any cracking. As a frame of reference, loads as small as 10 g could produce cracks in the single-phase $TiCr_2$ alloys. Some investigators have noted the critical load which initiates cracking as a significant parameter [49].

The room-temperature fracture toughness of the Cr-rich, bcc + $TiCr_2$ alloys were measured to be in the range of 5.0–6.5 MPa $m^{1/2}$ by this indentation technique. These values are far improved compared with the single-phase $TiCr_2$ alloys, which had toughness values of 0.75–1.5 MPa $m^{1/2}$. The two-phase Ti-rich and Cr-rich alloys with low volume fractions of $TiCr_2$ did not have appreciable cracking with indentation, and thus are expected to have even larger fracture toughness values.

High magnification SEM images of the indentation radial cracks showed that the crack paths were not necessarily straight, sometimes becoming more tortuous near the end of the crack tip. The two different phases obviously affect the crack path, and may disrupt the propagation of the crack. Cracks may be deflected at the matrix/precipitate interface, or decohesion of the bcc and the Laves phase may occur. Ashby et al. [33] have reasoned that the interface must be weak enough to debond in order to maximize the deformation of the ductile phase. Similar arguments have been presented for fiber-reinforced composites. Several other materials systems have been shown to be toughened by a second, more ductile phase by interface debonding and crack bridging, branching, deflection, and blunting.

Fracture toughness values of other two-phase Laves systems fall within the same range observed in this work for the two-phase $TiCr_2$ alloys. Bewlay et al. [18] report a fracture toughness of 3.1 MPa $m^{1/2}$ for Nb + $NbCr_2$ and 3.6 MPa $m^{1/2}$ for Cr + $NbCr_2$ alloys. Ravichandran et al. [50] report toughness values of 5–7 MPa $m^{1/2}$ for Cr + $HfCr_2$ alloys. Kumar and Miracle [21] achieved a fracture toughness of 7 MPa $m^{1/2}$ with Cr + $HfCr_2$ by notched 3-point bend test. However, this eutectic alloy had a fairly low volume fraction of the $C14$ $HfCr_2$ Laves phase. Cracks were seen along the interface and an extensive plastic zone was found ahead

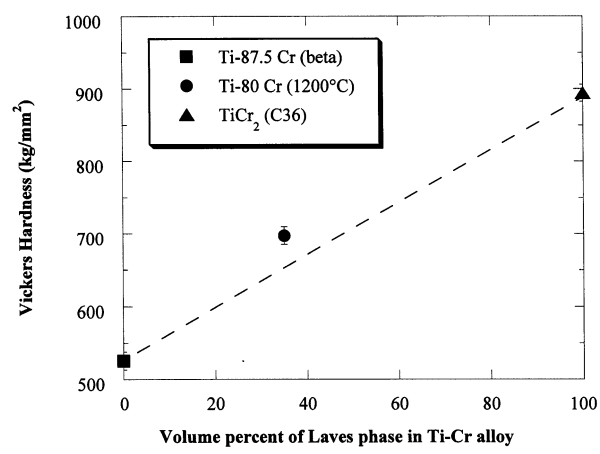

Fig. 9. Vickers hardness of Cr-rich, two-phase alloys as a function of the volume percent of Laves phase. The dotted line represents the rule of mixtures between the Cr-rich β-phase and single-phase ($C36$) $TiCr_2$.

of the crack tip, indicating similar deformation behavior as the two-phase bcc + $TiCr_2$ alloys.

Although comparisons of two-phase Laves systems are difficult because toughness is strongly dependent upon the Laves phase volume fraction, microstructure, and the test method, all the reported toughness values were below 10 MPa $m^{1/2}$. Bewlay and Jackson [51] place an upper limit of 10 MPa $m^{1/2}$ on Nb + $NbCr_2$ alloys that are alloyed with Hf and Ti, and in general, this limit currently holds true for all Laves phase systems at the time of writing of this paper.

4. Summary and conclusions

Several different factors affecting the mechanical properties of $TiCr_2$-base Laves phase alloys have been assessed. Defects companying the off-stoichiometric, Ti-rich $TiCr_2$ compositions (anti-site substitutions and Cr-site vacancies) are associated with a decrease in hardness and increase in fracture toughness values. These results lend credence to the postulate that vacancies play an important role in the movement of Shockley partial dislocations involved in the synchroshear deformation process. The vacancies (i.e. the removal of atoms) allow for easier atomic shifting within the close-packed Laves structure, which results in greater deformability. However, the increases in the toughness with off-stoichiometric $TiCr_2$ compositions are quite small, and other factors can have a stronger influence on the toughness.

The Laves phase crystal structure was also determined to be a significant factor affecting the mechanical properties of $TiCr_2$. The $C15$ structure in the binary and ternary $TiCr_2$-base Laves phases consistently displayed the highest hardness and fracture toughness values. Alloys with a $C36/C15$ structure showed no evidence of phase (crystal structure) transformation toughening, as exhibited by the $ZrFe_2$ Laves phase system. The greater deformability seen in the cubic $C15$ alloys over the hexagonal alloys can be attributed to the greater number of slip systems, as well as the ability to twin as an additional deformation mechanism.

Exclusive partitioning of alloying elements to either the A-sublattice (with Nb additions) or the B-sublattice of $TiCr_2$ (with Fe additions) resulted in decreases in the toughness. Mo and V additions to $TiCr_2$ exhibited some improvements, and these results suggest that large solubility of the appropriate alloying element can improve the toughness of the Laves phases. Furthermore, the study of ternary $TiCr_2$-base alloys revealed that alloying elements may be selected to stabilize the cubic $C15$ structure or to affect the single-phase solubility limit as additional alloying toughening strategies.

Overall, this work on $TiCr_2$-base alloys confirms the general thought that Laves phases are much too brittle at ambient temperatures to be used in their monolithic form, and if Laves phases are to ever find a practical application for structural purposes, they will most likely be in a two-phase system. The largest influence on the toughness of $TiCr_2$ was the presence of a second, more ductile phase. Even small amounts of the β-bcc phase with the $TiCr_2$-base intermetallics resulted in noticeable improvements in the fracture toughness. Through the proper choice of alloy composition and annealing treatments, microstructural design and control is possible with two-phase alloys containing $TiCr_2$. The Cr-rich, two-phase alloys displayed fracture toughness values about five to seven times larger than the single-phase alloys. The Ti-rich, two-phase alloys did not experience any indentation cracking and are expected to have an even larger fracture toughness, although the strength may be compromised. Improvements in the fracture toughness of the two-phase alloys can be attributed to crack deflection, crack bridging, and β-phase/$TiCr_2$ interface debonding. Thus, the deformability and toughness of $TiCr_2$ alloys greatly improve with a two-phase structure. The development of Laves phase alloys would best be approached by a combination of selecting the appropriate Laves phase composition (for sufficient toughness) and optimizing the microstructure of two-phase systems.

Acknowledgements

This research has been supported by the Division of Materials Sciences, Office of Basic Energy Sciences, United States Department of Energy, grant # DE-FG02-90ER45426. Dan J. Thoma is much appreciated for his useful discussions and comments.

References

[1] J.D. Livingston, Phys. Stat. Sol. (a) 131 (1992) 415.
[2] J.D. Livingston, E.L. Hall, J. Mater. Res. 5 (1990) 5.
[3] D.B. Miracle, Acta Metall. Mater 41 (1993) 649.
[4] T. Muller, P. Paufler, Phys. Stat. Sol. (a) 40 (1977) 471.
[5] P.J. Fehrenbach, H.W. Kerr, P. Niessen, J. Crystal Growth 18 (1973) 151.
[6] Z.B. Liu, L.C. Tai, J. Appl. Phys. 52 (1981) 2064.
[7] D.J. Thoma, Ph.D. Thesis, University of Wisconsin, 1992.
[8] T. Takasugi, M. Yoshida, S. Hanada, Acta Mater. 44 (1996) 669.
[9] K. Inoue, K. Tachikawa, IEEE Trans. Magn. 13 (1977) 840; 15 (1979) 635.
[10] F. Chu, D.P. Pope, MRS Proc. 288 (1992); Mater. Sci. Eng. A170 (1993) 39.
[11] Y. Liu, S.M. Allen, J.D. Livingston, Metall. Trans. 23A (1992) 3303.
[12] S. Mazdiyasni, D.B. Miracle, MRS Proc. 194 (1990) 155.
[13] W. Wunderlich, L. Machon, G. Sauthoff, Z. Metallk. 83 (1992) 679.

[14] M.P. Brady, J.L. Smialek, D.L. Humphrey, MRS Proc. 364 (1995) 1309.
[15] D.L. Anton, D.M. Shah, MRS Proceedings 194 (1990) 45.
[16] T. Takasugi, S. Hanada, K. Miyamoto, J. Mater. Res. 8 (1993) 3069.
[17] M. Takeyama, C.T. Liu, Mater. Sci. Eng. A132 (1991) 61.
[18] B.P. Bewlay, J.A. Sutliff, M.R. Jackson, H.A. Lipsett, Acta Metall. Mater. 42 (1994) 2869.
[19] C.T. Liu, P.F. Tortorelli, J.A. Horton, C.A. Carmichael, Mater. Sci. Eng. A214 (1996) 23.
[20] V.M. Azhazha, A.P. Berdnik, A.P. Svinarenko, A.I. Somov, Flz. Metal. Metalloved. 41 (1976) 402.
[21] K.S. Kumar, D.B. Miracle, Intermetallics 2 (1994) 257.
[22] K.C. Chen, S.M. Allen, J.D. Livingston, MRS Proc. 288 (1992) 373.
[23] G. Sauthoff, Z. Metallk. 80 (1989) 337.
[24] R.L. Fleischer, R.J. Zabala, Metall. Trans. 21A (1990) 2149.
[25] D.J. Thoma, J.H. Perepezko, J. Alloys Compounds 224 (1995) 330.
[26] K.C. Chen, S.M. Allen, J.D. Livingston, J. Mater. Res. 12 (1997) 1472.
[27] G.R. Anstis, P. Chantikul, B.R. Lawn, D.B. Marshall, J. Am. Ceram. Soc. 64 (1981) 533.
[28] H.E. Exner, Trans. Met. Soc. AIME 245 (1969) 677.
[29] K.C. Chen, S.M. Allen, J.D. Livingston, MRS Proc. 364 (1994) 1406.
[30] K.C. Chen, Ph.D. Thesis, MIT, 1996.
[31] J.H. Westbrook, in: J.H. Westbrook (Ed.), Mechanical Properties of Intermetallic Compounds, Wiley, New York, 1960.
[32] P. Paufler, K. Eichler, G.E.R. Schulze, Monatsberichte 12 (1970) 949.
[33] P. Paufler, Chemische Gesellschaft 9 (1984) 175.
[34] P.M. Hazzledine, K.S. Kumar, D.B. Miracle, A.G. Jackson, MRS Proc. 288 (1992) 591; P.M. Hazzledine, P. Pirouz, Scr. Metall. 28 (1993) 1277.
[35] M.F. Ashby, F.J. Blunt, M. Bannister, Acta Metall. 37 (1989) 1847.
[36] F. Laves, H. Witte, Metallwertschaft 15 (1936) 840.
[37] W.B. Pearson, Crystal Chemistry and Physics of Metals and Alloys, Wiley-Interscience, New York, 1972.
[38] A.R. Edwards, Metall. Trans. 3 (1972) 1365.
[39] I.I. Kornilov, N.G. Boriskina, Zhur. Neorg. Khim. 9 (1964) 702.
[40] R.J. Van Thyne, H.D. Kessler, M. Hansen, Trans. AIME 197 (1953) 1209.
[41] I.I. Kornilov, K.I. Shakhova, P.B. Budberg, N.A. Nedumov, Doklady Akademi Nauk SSSr 149 (1963) 1340.
[42] F. Chu, D.J. Thoma, P.G. Kotula, S. Gerstl, T.E. Mitchell, I.M. Anderson, J. Bentley, Acta Met., in press.
[43] R.L. Fleischer, Structural Intermetallics, in: R. Darolia, J.J. Lewandowki, C.T. Liu, P.L. Martin, D.B. Miracle, M.V. Nathal (Eds.), TMS, Warrendale, Pennsylvania, 1993, p. 691.
[44] R.L. Berry, G.V. Raynor, Acta Cryst. 6 (1953) 178.
[45] W.B. Pearson, Acta Cryst. B37 (1981) 1174.
[46] R.L. Fleischer, Scr. Metall. Mater. 27 (1992) 799.
[47] E.P. George, C.T. Liu, MRS Proc. 196 (1991) 309.
[48] S. Zhang, J.P. Nic, D.E. Mikola, Scr. Metall. Mater. 24 (1990) 57; 24 (1990) 1099.
[49] J.P. Nic, S. Zhang, D.E. Mikkola, Scr. Metall. Mater. 24 (1990) 1099.
[50] K.S. Ravichandran, D.B. Miracle, M.C. Mendiratta, MRS Proc. 350 (1994) 249.
[51] B.P. Bewlay, M.R. Jackson, J. Mater. Res. 11 (1996) 1917.